CHAPTER 4

ELECTROCHEMICAL MODEL FOR GRAPHENE ENFET (G-ENFET) WITH ZrO_2 AS DIELECTRIC FOR CHOLESTEROL DETECTION

CHAPTER 4

Electrochemical model for graphene ENFET (G-ENFET) with ZrO_2 as dielectric for cholesterol detection

4.1. An overview on G-ENFET

G-ENFET is an ENFET device in which graphene nanomaterial is used as substrate semiconductor. Graphene has a 2-D structure with tunable band gap property. The band gap of the graphene semiconducting channel depends on its width. More the width of graphene, higher is the mobility [39]. It displays a very high mobility with a large surface area. It remains mechanically and chemically stable, which makes its fabrication easier and better. It also has a high compatibility with high-κ dielectrics. All these extraordinary properties of graphene resulted into the development of G-ENFET pushing the semiconductor industry a step closer towards nano-level miniaturized biosensors with improved performance. Moreover, graphene–CNT combined FET also, exhibits excellent device performances with significant reduction in hysteresis, better output, high flexibility, and stretch-ability [13]. The highly biocompatible CNTs makes them promising for holding enzymes.

As discussed in Chapter 2, cholesterol is a soft and waxy fat that our body needs to function properly. However, high level of cholesterol in the blood may cause disorders such as hypertension, atherosclerosis, nephrosis, myxedema, jaundice and myocardial infarction. Similarly, low level of cholesterol may result in hyperthyroidism, anaemia and mal adsorption. Therefore, detection of cholesterol is very important. Thus, this chapter presents the electrochemical modeling of Potassium-doped Polypyrrole/Carbon Nanotube (K/PPy/CNT) based G-ENFET for detection of cholesterol. The details of fabrication and characterization of this sensor is given in reference [8]. Since, values of parameters used for modeling this device has been extracted mostly from parameters used for fabrication of the device and the experimental results, a brief description of its fabrication process and the experimental part has been highlighted in the next section. The schematic of the fabricated G-ENFET is shown in Fig. 4.1. It consists of indium tin oxide (ITO) coated glass as bottom substrate, high-κ dielectric ZrO_2 as bottom insulator, boron doped p-type graphene as substrate, nitrogen doped n-type graphene as

source and drain regions, high-κ dielectric ZrO_2 as gate insulator and K/PPy/CNT composite as sensing membrane on the top of ZrO_2 layer. The structure of B-doped and N-doped graphene has been shown in Chapter 2. The structure of formation of K/PPy/CNT composite with ZrO_2 has been shown in Fig. 4.2.

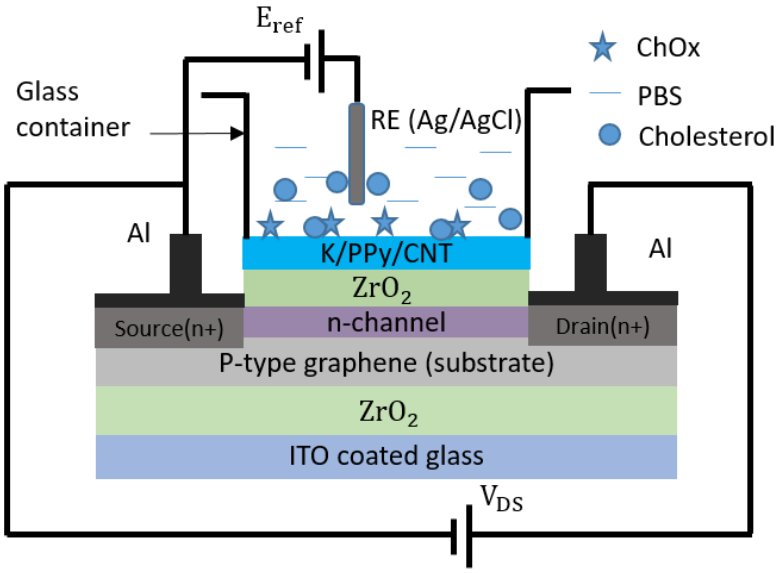

Fig. 4.1. Schematic of fabricated G-ENFET for Cholesterol Detection [8]

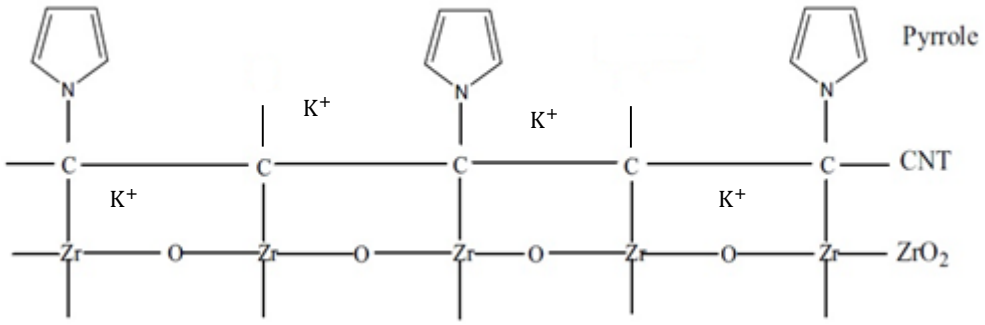

Fig. 4.2. Structure of formation of K/PPy/CNT composite with ZrO_2 [8]

4.2. Fabrication and characterization of G-ENFET

The fabrication of G-ENFET has been done using chemical solution process as discussed in Chapter 2. Firstly, ITO coated glass plate having sheet resistance ~15 Ω /cm^2 and dimension: 11 mm x 5 mm has been used as substrate material. On the top of

ITO, a layer of ZrO_2 has been deposited to prevent leakage current from channel to ITO. To deposit this layer, 5.0 mg solid zirconium tetra-chloride ($ZrCl_4$) has been hydrolyzed in 5 ml water (H_2O) and sonicated for 15 to 25 minutes. Using ECD technique, a thin layer of ZrO_2 has been deposited on ITO glass and heated at a temperature of 180°C to dry out. The thickness of this layer does not matter, since it is not a gate insulator. On the top of the ZrO_2 layer, p-type graphene layer (dimension: 11 mm x 5 mm x 100 nm) has been deposited using ECD technique. This layer acts as substrate for n-channel FET. P-type graphene has been prepared by doping 2 µl of BBr_3 (1 M) in 100 µl of graphene (1 M), and hydrogen gas has been blown through the solution (resulting p-type substrate with N_D~20%, N_A~10%, work function~5.5eV) [24, 38]. Similarly, nitrogen (N_2) gas has been blown by gas flow sputtering at normal temperature and pressure for making n-type source (S) and drain (D) (work function~3.10 eV) [85]. For the simplicity of biomolecule immobilization, the channel length (L) and width (W) have been chosen equal to ~ 1mm and ~5 mm, respectively. On the channel region, another layer of ZrO_2 has been deposited as gate insulator of the FET. This layer is deposited only on the channel region, so, the area for source and drain contact is masked using Teflon tape [29]. The dimension of this layer is ~ 1 mm × 5 mm × 10 nm. ZrO_2 (high κ-dielectric ~25) deposited on the channel region increases the capacitance of the gate insulator and hence, sensitivity of FET. The thickness of the gate insulator has been measured using gravimetric analysis method discussed in Chapter 2.

To make contacts on both source and drain regions, Aluminium (Al) metal has been deposited using filament evaporation technique. On the top of the gate insulating layer, a sensing membrane is to be deposited for ChOx immobilization. This sensing membrane has been prepared as: 5 mg of CNT has been added in 5 ml acetonitrile and sonicated for 10 min for preparation of CNT solution. 2 ml of KOH solution (1 M) (as potassium is unstable in air and very reactive with water) has been added in 10 µl CNT solutions for preparation of K-doped CNT solution; 8 µl pyrrole (1 mg/ml in formic acid) solution with 10 µl K-doped CNT solution has been added in 10 ml acetonitrile. In this way, composite solution of K-doped CNT/PPy has been prepared and deposited on top of ZrO_2 by using ECD technique (K~20%/PPy~50%/CNT~100%)~6.5eV, work functions of K~2.3eV, PPy~5.2eV and CNT~4.9eV). The dimension of this layer has been taken as ~ 1 mm × 5 mm × 50 nm. The biocompatibility of CNT is very high and

doping with potassium increases its density of free charge carriers in addition to electrical and thermal conductivity. Also, addition of polypyrrole enhances the dispersion property of CNTs.

Referring to experimental part, experiments need to be performed to see the gate dependence similarity of the device both outside (G-MOSFET) and in-liquid (G-ENFET) measurements.

For the measurements outside the liquid: aluminum metal (work function 4.08 eV) has been deposited on the top of the ZrO_2 layer (by filament evaporation technique) that acts as the gate of MOSFET forming G-MOSFET. Experiments have been performed to find the output and transfer characteristics of the device outside the liquid. For output characteristic curves, dc drain currents measured by digital multimeter (DMM) have been plotted against drain voltages from 0 to 1 V, in step of 0.2 V with some applied gate voltages from 0 to 1 V, in step of 0.2 V as shown in Fig. 4.3. Similarly, the transfer characteristic curve has been drawn (for $V_{DS} = 0.3\,V$) as shown in Fig. 4.4. The threshold voltage from the transfer characteristic curve has been obtained by using extrapolation in linear region method (ELR) and found as ~ 0.18V.

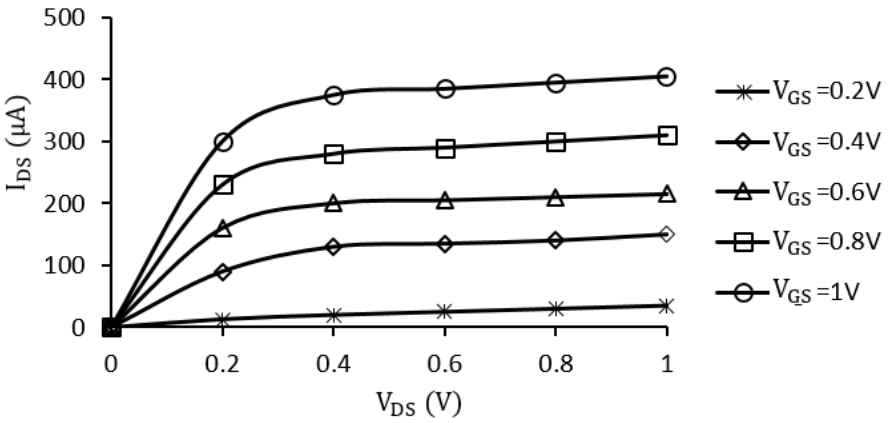

Fig. 4.3. Output characteristics of G-MOSFET

For in liquid measurements (G-ENFET): ChOx with ~ 24 U/mg activity has been purchased from Sigma Aldrich (USA). ChOx solution (1mg/ml) has been prepared using phosphate buffer saline (PBS). PBS having 50 mM, pH 7.0 has been prepared using sodium monophosphate (Na_2HPO_4) and sodium diphosphate (NaH_2PO_4) with

0.9% NaCl and used as mediator. 1 µl of ChOx solution has been immobilized onto K/PPy/CNT layer of FET using physical adsorption technique, then dried overnight under desiccated conditions and washed with PBS to remove any unbound ChOx and stored at 4°C when not in use.

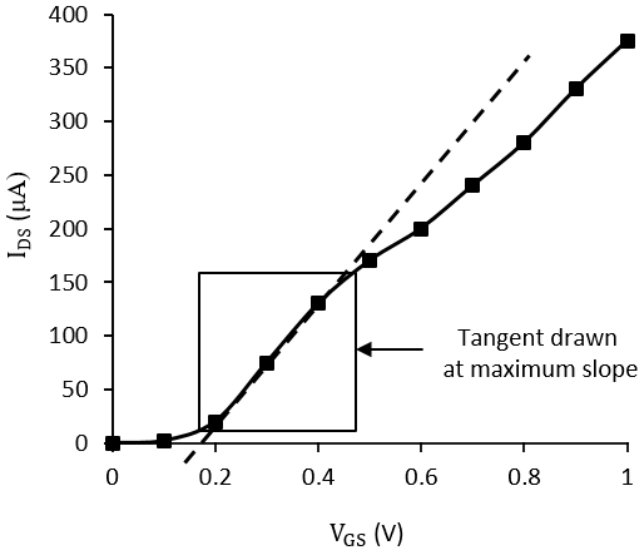

Fig. 4.4. Transfer characteristics of G-MOSFET to extract $V_{TH,G-MOSFET}$ using ELR technique

Cholesterol (powder form) with 99% purity was purchased from Sigma Aldrich. Though cholesterol is not dissolved in water, it can be blended with some other substances. Here, cholesterol stock solutions with different concentrations (0.5 mM to 25 mM) have been prepared using 2% Triton X-100 as surfactant. For instance, for preparing cholesterol stock solution of 5 mM, 100 mg cholesterol is dissolved in a 2 mL Triton X-100. This mixing process involves boiling, sonication and filtration. The solution is then stored at 4°C in the dark and stable for about two weeks (until a slight turbidity is observed).

To measure electrical response, the G-ENFET with reference electrode (Ag/AgCl) has been inserted in a glass pot containing 20 ml PBS (50 mM, pH 7.0). A potential in the range from 0 to 0.4 V in steps of 0.1 V has been applied between source and drain where positive and negative supply have been connected to drain and source, respectively. Similarly, a fixed potential 0.7 V has been applied between reference electrode and source where positive and negative supplies have been connected to reference electrode and source, respectively. A digital multimeter (Agilent 3458A) has been used to

measure drain current (I_{DS}). 10 µl stock solution of cholesterol (concentration from 0.5 to 25 mM) has been added by micropipette to PBS in the pot each time, and corresponding drain current against each cholesterol concentration has been recorded by digital multimeter.

The drain current (I_{DS}) and drain voltage (V_{DS}) for cholesterol concentration (0.5 to 25 mM) have been plotted as shown in Fig. 4.5. It has been observed that up to potential of 0.2 V, drain current is linear and then, it saturates just like characteristic curves of a MOSFET. It was found that the device has linearity for detection of cholesterol concentration from 0.5 to 20 mM.

In MOSFET device, threshold voltage is constant (It is kept constant through well-controlled fabrication process). Its transfer characteristics (V_{GS} vs I_{DS}) is drawn keeping V_{DS} at a constant value. Unlike MOSFET, ENFET is a pH or concentration dependent threshold voltage controlled device. Its transfer characteristics can, therefore be experimentally determined using any of the following two methods:

i. Keeping pH (and hence, concentration of electrolyte solution being measured) and V_{DS} constant, I_{DS} can be recorded by varying V_{GS}, i.e. V_{GS} vs I_{DS} curve.

ii. Keeping both V_{DS} and V_{GS} constant (at which values these are to be fixed can be determined from linearity curve), the transfer characteristic curve can be drawn between pH (or concentration) and I_{DS} as pH here serves as an input parameter.

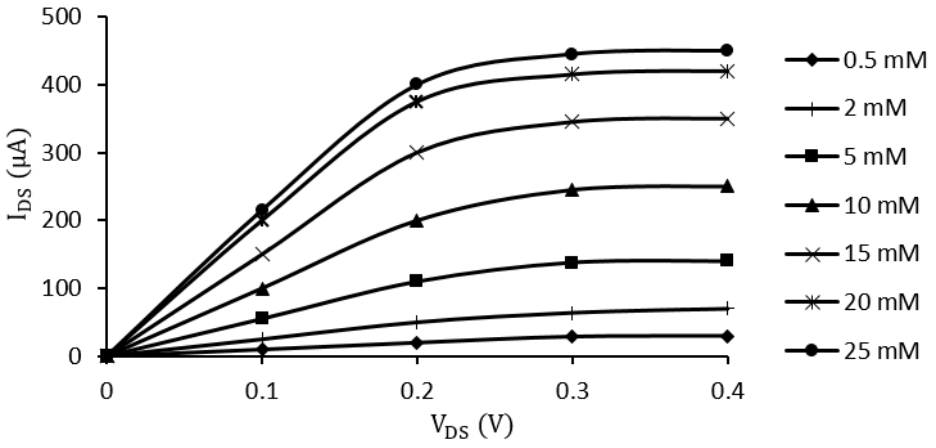

Fig. 4.5. Output characteristics of G-ENFET

Here, the first method is used, when threshold voltages at different pH values of electrolyte solution are desired. Considering the G-ENFET, the transfer characteristic curves of the device have been plotted experimentally for cholesterol solution of different concentration having pH 5.5 and 6 (plot for only two pH values are displayed for clarity of graph) keeping V_{DS} = 0.2 V. The variation of ENFET threshold voltage with change in pH of cholesterol solution was then determined from these V_{GS} vs I_{DS} curves using ELR technique as shown in Fig. 4.6.

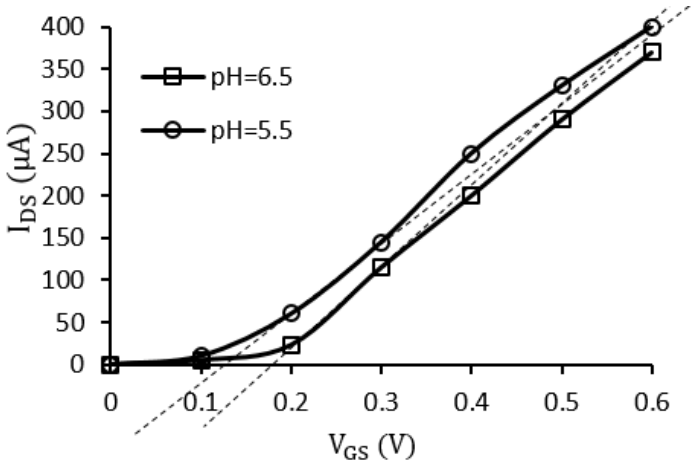

Fig. 4.6. Transfer characteristics of G-ENFET

4.3. G-ENFET MODEL

The modeling of G-ENFET is done following the generalized electrochemical model. To start the modeling, the whole device is taken along the diffusion length (x) as the horizontal axis with ZrO_2 as shown in Fig. 4.7.

The modeling is done using the enzymatic reactions of the enzyme cholesterol oxidase on cholesterol substrate, diffusion phenomena of the main substrate (i.e. cholesterol) in phosphate buffer saline (PBS), acid/base reactions of the product (H_2O_2) in the PBS solution (pH=7) , pH detection properties of ISFET and current transport model of G-ENFET.

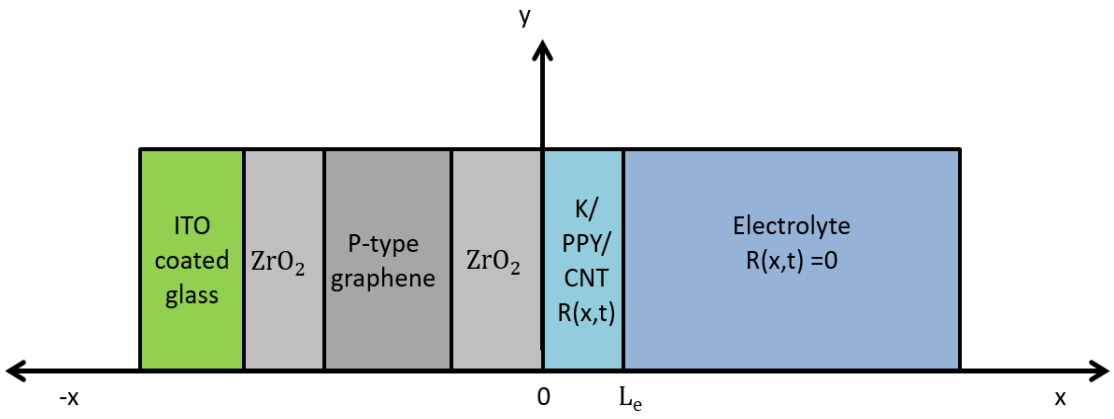

Fig. 4.7. Description of G-ENFET structure with respect to diffusion length (x)

4.3.1. Modeling of cholesterol oxidase enzymatic reactions

The enzyme ChOx catalyzes the reaction of cholesterol in the presence of O_2 into formation of Cholest-4-en-3-one and H_2O_2 as shown in Eq. (4.1). The enzymatic reaction is modeled by using Michaelis–Menten equation as shown in Eq. (3.8) of Chapter 3.

$$Cholesterol + O_2 \xrightarrow{ChOx} Cholest - 4 - en - 3 - one + H_2O_2 \quad (4.1)$$

Cholesterol and Cholest-4-en-3-one do not have any acid/basic properties, so, they do not intervene in ENFET detection by pH variations. It is found that the product H_2O_2 only contributes towards the acid/base reactions at the electrode as it releases H^+ ions. So, in further calculations cholesterol is takes as substrate and H_2O_2 is taken as product.

4.3.2. Modeling of diffusion of cholesterol and H_2O_2 in PBS solution

The modeling has been done using the diffusion model discussed in Section 3.2.2 of Chapter 3 taking $[S]$ = cholesterol concentration and $[P]$ = H_2O_2 concentration. To determine the diffusion constants as shown in Eq. (3.11) of Chapter 3, the fluid dependent constant (A_f) need to be calculated. The fluid for this device is the electrolyte i.e. PBS solution. Phosphate buffered saline (PBS) is a buffer solution commonly used in the field of biological and biomedical research. It is a salty solution

containing sodium chloride (NaCl), potassium chloride (KCl), sodium hydrogen phosphate (Na_2HPO_4) and potassium dihydrogen phosphate (KH_2PO_4). The buffer helps to maintain a constant pH.

Considering the composition of PBS to be 1 X, the volumic mass can be calculated as given under

Salt	Concentration (m mol/L)	Concentration (g/L)
NaCl	137 X	8.0 X
KCl	2.7 X	0.2 X
Na_2HPO_4	10 X	1.42 X
KH_2PO_4	1.8 X	0.24 X
Total	151.5 X = 50 mM ⇒ X= 0.33	9.86 X = 3.25 g/L

Thus, the volumic mass (ρ) of 50 mM PBS solution is obtained as 3.25 g/L. The viscosity (η) of PBS solution at room temperature is 10.5×10^{-3} gm/cm s. Using these values, the value of A_f for PBS solution is obtained as $1.0185\times10^{9}\ \mathrm{g^{-1}cm\ s}\sqrt[3]{\mathrm{g\ mol^{-1}L^{-1}}}$. The molar mass of cholesterol and H_2O_2 are 386 g/mol and 34.0147 g/mol respectively. Thus, D_S(cholesterol) and D_P(H_2O_2) are found to be 5.788×10^{-7} $cm^2\ s^{-1}$ and 1.3014×10^{-6} cm^2s^{-1} respectively as shown in Table 4.2. Using these diffusion constants in the diffusion model as given by Eqs. (3.9) and (3.10) of Chapter 3, the substrate and product variations in the enzyme layer with diffusion length was obtained as shown in Fig. 4.8. It is noticed from the graph that from L_e to 0, substrate concentration decreases and product concentration increases as we approach the insulator surface. Beyond the enzyme layer i.e. deep into the bulk electrolyte the substrate concentration is constant and product concentration is almost zero. This shows consumption of cholesterol and production of H_2O_2. As the time increases we see more substrate is consumed and product is formed at the enzyme –insulator interface.

Fig. 4.9 shows the substrate and product concentration variation with diffusion length at different enzyme layer thickness (10^{-5} to 4×10^{-5} cm). As seen in the graph, more the diffusion length, lesser is the substrate concentration and higher is the product concentration. This is because an increase in diffusion length gives more substrate to

be inside the enzyme area. Higher the substrate biomolecules, higher is the product formation by the enzymes.

Fig. 4.10 shows the substrate and product concentration variation with the change in n_{enz}. It is seen that as the n_{enz} increases, the substrate is fully consumed. At n_{enz}=10^3 unit/cm^3, the substrate consumption is much less at the enzyme-insulator interface as compared to n_{enz} =10^5 unit/cm^3, where the substrate is almost fully consumed. This shows that the increase in enzymatic units because of greater holding capability of K/PPY/CNT composite layer has enabled more substrate consumption and thereby, product formation. This has resulted in the increase in sensitivity of the device. The graph was plotted for initial substrate concentration of 25mM and 100nm length of the enzyme layer.

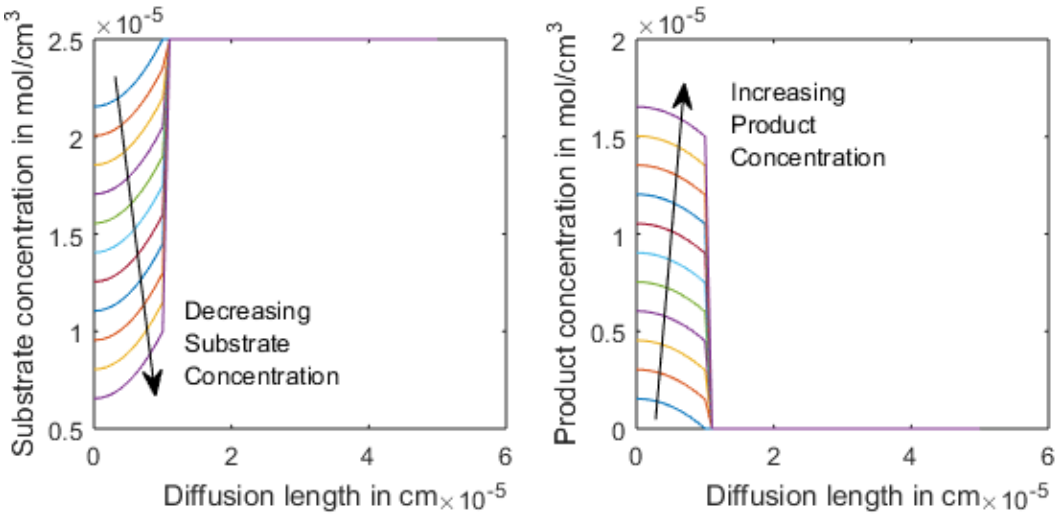

Fig. 4.8. Substrate and product concentration variation with diffusion length at different time

4.3.3. Modeling pH variations due to release of H^+ ions

The product, H_2O_2 releases H^+ ions at the electrode, which contribute towards the change in pH at the enzyme- insulator interface (Eq. (4.2)).

$$H_2O_2 \xrightarrow{Electrode} O_2 + 2H^+ + 2e^- \quad (4.2)$$

The H^+ ions that are produced forms physical bonds at the surface of ZrO_2 resulting in variations in pH. The concentration of H^+ions, which results in pH variations can be found out using the acidic equilibrium constant as shown in Eq. (4.3). The total concentration of H^+ ions is given by Eq. (4.4). Using this pH variations are found out as shown in Eq. (4.5).

$$K_a = \frac{[O_2][H^+]^2}{[H_2O_2]} \tag{4.3}$$

$$[H^+]_{total} = 2[H^+] + C_i \tag{4.4}$$

$$pH = -log[H^+]_{total} \tag{4.5}$$

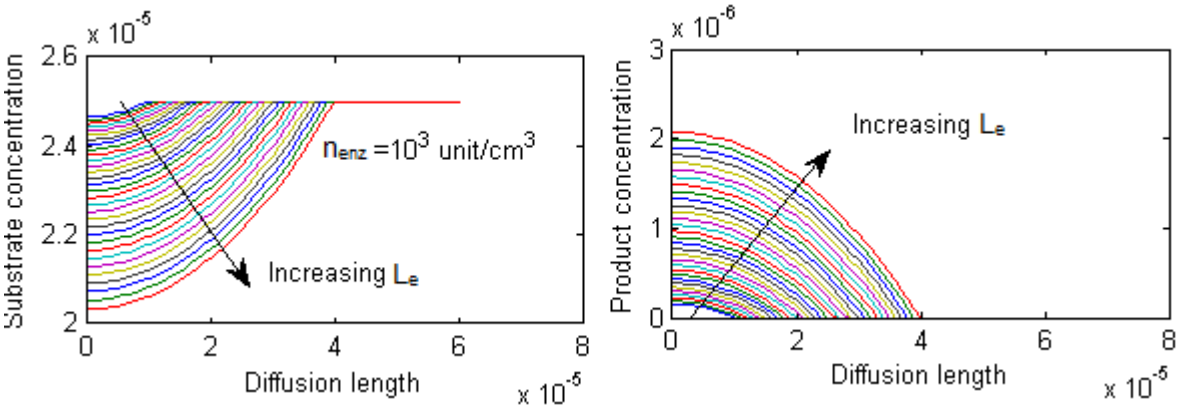

Fig. 4.9. Substrate and product concentration variation with diffusion length at different enzyme layer thickness (L_e)

where, C_i is the initial concentration of H^+ions present in the buffer solution having $pH_0 = 7$. Fig. 4.11. shows the variation of pH with the diffusion length. Here, it is seen that as the substrate concentration decreases and product concentration increases, the H^+ ion concentration increases resulting in decrease in pH at the insulator enzyme interface. The pH gradually decreases from 7 as it approaches the interface showing more acidic nature closer to the interface. When the H^+ ions concentration becomes much higher in the enzyme layer then the pH becomes almost constant throughout.

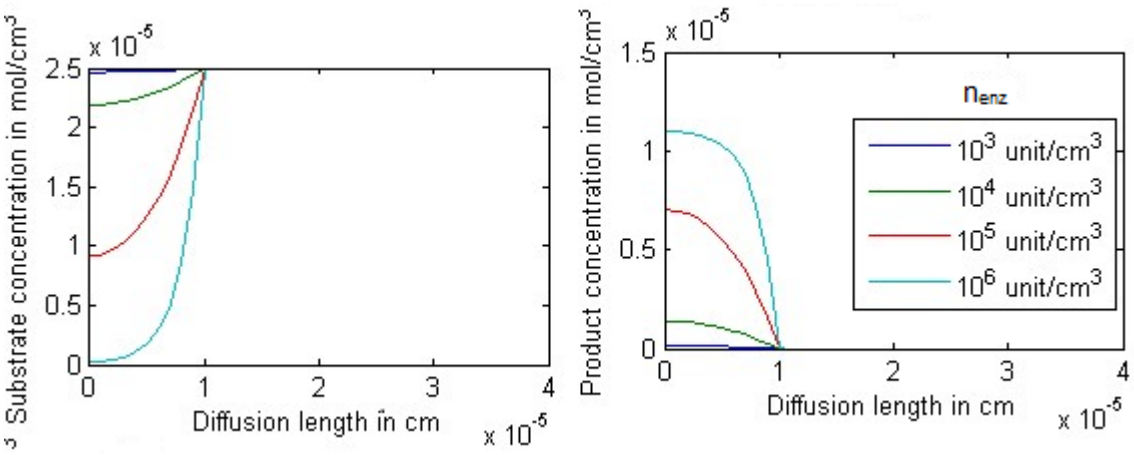

Fig. 4.10. Substrate and product concentration variation with diffusion length at different n_{enz} with L_e=10^{-5}cm.

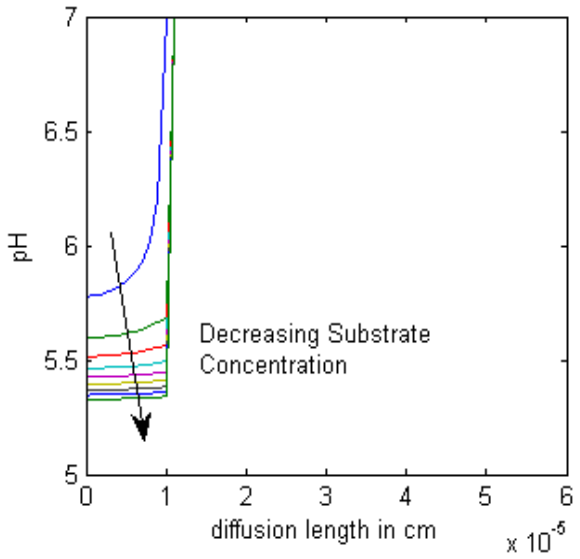

Fig. 4.11. Diffusion length vs pH with decreasing substrate concentration

4.3.4. Current transport model for G-ENFET

It is clear from the Fig. 4.5 that the fabricated G-ENFET behaves like a MOSFET. The current transport model for G-ENFET can, therefore, be obtained by modifications over the general current transport model of MOSFET. Using $V_{TH,G-ENFET}$, the threshold voltage for G-ENFET in the ENFET current equations shown in Eqs. (3.45) and (3.46)

of Chapter 3, the drain current equations for a G-ENFET in the linear and saturation regions has been obtained. Determination of $V_{TH,G-ENFET}$ is the important thing in the current transport model for G-ENFET. It is determined by using Eq. (4.6).

$$V_{TH,G-ENFET} = E_{ref} - \psi_{0,G-ENFET} + \chi_{sol} - \frac{\Phi_{graphene}}{q} - \frac{Q_{ox} + Q_{ss} + Q_{graphene}}{C_{ox}} + 2\Phi_f \tag{4.6}$$

where, χ_{sol} is the surface dipole potential of the solution, $\Phi_{graphene}$ is the work function of graphene, C_{ox} is the gate insulator capacitance, Q_{ox} is the insulator charge, Q_{ss} is the insulator semiconductor interface charge, $Q_{graphene}$ is the semiconductor depletion region charge in graphene, Φ_f is the Fermi potential of graphene and $2\Phi_f$ in the channel inversion potential. $\psi_{0,G-ENFET}$ is the surface potential, which is calculated using the Bousse's model shown in Eq. (2.13) of Chapter 2. The surface potential variation leads to the variation in threshold voltage (other parameters remaining constant).

The charge in the insulator has been found out using Eq. (4.7), where N_{ox} is the number of charge carriers present in the oxide layer. The fermi potential of graphene has been calculated using Eq. (4.8), where N_A is the concentration of acceptors and n_i is the intrinsic carrier concentration of graphene. The semiconductor depletion region charge in graphene has been found out using Eq. (4.9), where the permittivity of graphene is given by $\varepsilon_{graphene} = \kappa_{graphene}\varepsilon_0$. $\kappa_{graphene}$ is the dielectric constant for graphene and ε_0 is the permittivity of free space. The oxide capacitance per unit area has been found using Eq. (4.10), where κ is the dielectric constant of ZrO_2 and t_{ox} is its thickness.

$$Q_{ox} = qN_{ox} \tag{4.7}$$

$$\Phi_f = \frac{kT}{q}\log\frac{N_A}{n_i} \tag{4.8}$$

$$Q_{graphene} = -\sqrt{4\varepsilon_{graphene}qN_A\Phi_f} \tag{4.9}$$

$$C_{ox} = \frac{\kappa\varepsilon_0}{t_{ox}} \tag{4.10}$$

Experimentally, it is difficult to determine the surface potential. So, its experimental values are calculated using the relation given in Eq. (4.11).

$$V_{TH,G-ENFET} = V_{TH,G-MOSFET} - \psi_0 + \text{constant} \tag{4.11}$$

where, $V_{TH,G-MOSFET}$ value is obtained from the transfer characteristics shown in Fig. 4.4, $V_{TH,G-ENFET}$ values are obtained from the transfer characteristics shown in Fig. 4.6 at different pH and the other remaining parameters are taken as constant. Using these values the $\psi_{0,G-ENFET}$ for different pH can be obtained. A comparative plot of modeling and experimental results for $\psi_{0,G-ENFET}$ and $V_{TH,G-ENFET}$ have been shown in Fig. 4.12 A and B respectively. The results show good fit.

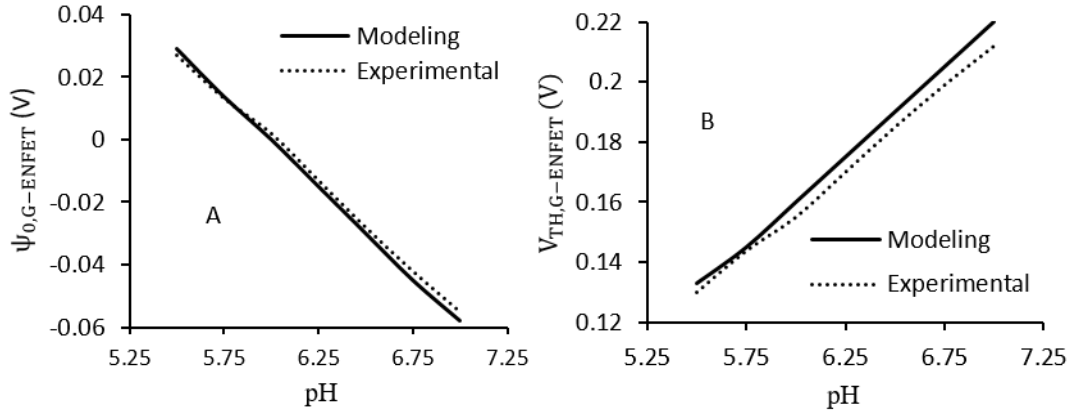

Fig. 4.12. (A) Comparison of modeling and experimental results for $\psi_{0,G-ENFET}$ vs pH

(B) Comparison of modeling and experimental results for $V_{TH,G-ENFET}$ vs pH

Using the current equations, the output characteristics of G-ENFET was found using $V_{TH,G-ENFET}$ at different pH or cholesterol concentrations. Fig. 4.13 shows a good fit between the modeling and experimental results at different cholesterol concentrations. The values of important parameters considered for G-ENFET modeling has been shown in Table 4.1.

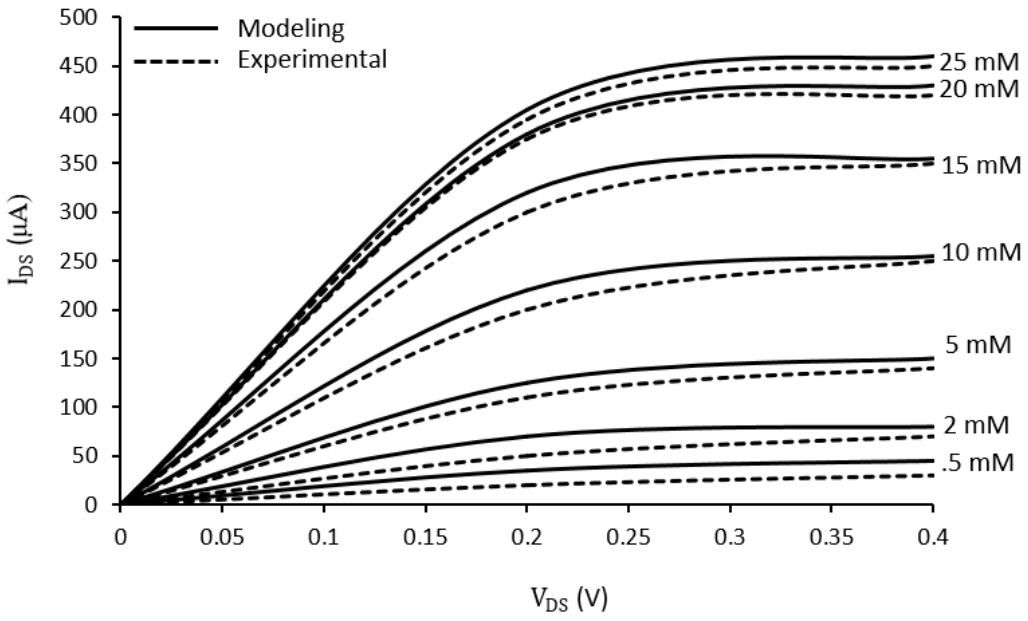

Fig. 4.13. Output characteristics of G-ENFET showing comparison between modeling and experimental results

4.4. Summary

The G-ENFET model has been developed for cholesterol detection using the enzymatic reactions, diffusion phenomena, acid/base reactions and the pH detection properties of ISFET. The ISFET consists of ZrO_2 as gate insulator on top of graphene substrate. ZrO_2 is a high-κ dielectric with dielectric constant 25 and has thickness of about 10 nm giving good insulating effect even at nanometer range. The K/PPY/CNT in which the enzymes are immobilized has larger area and lesser thickness of about 100 nm. As a result, it can hold more enzymes, give better response time and higher sensitivity. The mobility of graphene is very high (about 15000 cm^2/Vs). This also contributes towards the high sensitivity of the device as even very small potential variation at the surface gives a noticeable change in current. The results of the model show good agreement with the experimental results. This model helps to understand how ENFET works for cholesterol detection based on ISFET's pH measuring principle. Not only cholesterol, this model can also be used for other enzyme – analyte combinations.

Table 4.1. Values of important parameters considered for G-ENFET modeling

Sl. No.	**Parameter**	**Values**
1.	Maximal enzyme activity (a_M)	16.67×10^{-9} mol/s for 1 ChOx unit
2.	Number of enzymatic units per unit volume (n_{enz})	24×10^5 ChOx units/cm^3
3.	Michaelis Menten Constant (K_M)	2.5 mM
4.	Cholesterol diffusion constant (D_S)	5.788×10^{-7} cm^2/s
5.	H_2O_2 diffusion constant (D_P)	1.3014×10^{-6} cm^2/s
6.	Enzyme layer thickness (L_e)	100 nm
7.	Acid dissociation constant for H_2O_2 (K_a)	2.5×10^{-12}
8.	Reference Voltage (E_{ref})	0.7 V
9.	Dielectric constant for ZrO_2 (κ)	25
10.	Dielectric constant for graphene ($\kappa_{graphene}$)	2.3
11.	pH of PBS solution (pH_0)	7
12.	pH_{pzc} for ZrO_2	6
13.	Surface dipole potential of the solvent (χ_{sol})	0.3 V
14.	Electron mobility of graphene (μ)	15000 cm^2/Vs
15.	Carrier concentration in oxide layer (N_{ox})	3×10^{10} cm^{-2}
16.	Concentration of acceptors (N_A)	5×10^{18} cm^{-3}
17.	Intrinsic carrier concentration of graphene (n_i)	9×10^{10} cm^{-3}
18.	Thickness of ZrO_2 layer (t_{ox})	10 nm
19.	Work function of graphene ($\phi_{graphene}$)	4.5 eV
20.	Permittivity of free space (ε_0)	8.85×10^{-14} F/cm
21.	Temperature (T)	25 °C
22.	Elementary charge (q)	1.6×10^{-19} C
23.	Width of channel (W)	5 mm
24.	Length of channel (L)	1 mm